EUROPEAN ORGANIZATION FOR NUCLEAR RESEARCH

CERN-PPE/92-87
29 May 1992

A Test of Quantum Electrodynamics in the Reaction $e^+e^- \rightarrow \gamma\gamma(\gamma)$

L3 Collaboration

ABSTRACT

We have measured the total and differential cross sections of the reaction $e^+e^- \rightarrow \gamma\gamma(\gamma)$ at center-of-mass energies around 91 GeV, with an integrated luminosity of 14.2 pb^{-1}. The results are in good agreement with QED predictions. We set lower limits, at 95% confidence level, on the QED cutoff parameters of $\Lambda_+ >$139 GeV, $\Lambda_- >$108 GeV and on the mass of an excited electron of $m_{e^*} >$127 GeV. We searched for Z^0 rare decays with photonic signatures in the final state. Upper limits, at 95% confidence level, for the branching ratio of Z^0 decaying into $\pi^0\gamma/\gamma\gamma$, $\eta\gamma$ and $\gamma\gamma\gamma$ are 1.2×10^{-4}, 1.8×10^{-4}, 3.3×10^{-5} respectively.

Submitted to Physics Letters B

1 Introduction

Quantum Electrodynamics (QED) is the best tested theory in physics; so far no deviation has been found even at small distances. The reaction $e^+e^- \rightarrow \gamma\gamma(\gamma)$ is a pure QED process and can test breakdown effects. QED breakdown would imply that the electron has a finite size [1–3]. In particular an excited electron might exist which couples to electrons and photons with a magnetic interaction: $\frac{e\lambda}{2m_{e^*}}\overline{\psi_{e^*}}\sigma_{\mu\nu}\psi_e F^{\mu\nu}$ where m_{e^*} is the mass of the excited electron, λ the coupling constant and $F^{\mu\nu}$ the electromagnetic field tensor [2]. This interaction is gauge invariant but is not renormalizable and the effect of such a breakdown has been parametrized [1,2]. The total differential cross section at the Born level, $(d\sigma/d\Omega)^0_T$, can be written as:

$$(d\sigma/d\Omega)^0_T \equiv \sigma(\theta)^0_T = \sigma(\theta)^0_{QED}\,(1 \pm \delta_{new})$$

where $\delta_{new} = s^2/2\,\left(1/\Lambda^4_\pm\right)\,(1-\cos^2\theta)$, θ is the angle of the emitted photons with respect to the beam axis, $\sqrt{s}$ the center-of-mass energy and $\Lambda_\pm$ the QED cut-off parameters.

The reaction $e^+e^- \rightarrow \gamma\gamma(\gamma)$ can also be used to search for forbidden or rare Z^0 decays with photons in the final state. Since Z^0 is a spin 1 boson it is not allowed to decay into two photons [4]. Some models predict a coupling of Z^0 to $\pi^0\gamma$ or $\eta\gamma$ [5]. The decay of Z^0 to three photons has a branching ratio in the Standard Model of about 7×10^{-10} [6]. However in some compositeness models branching ratios as high as 10^{-4} are predicted [7,8].

We have previously published the results of the reaction $e^+e^- \rightarrow \gamma\gamma(\gamma)$ based on 32 events [9]. Similar results have been published by other experiments [12]. With our latest data, corresponding to an integrated luminosity of 14.2pb^{-1} and an improved acceptance, we have increased the statistics by an order of magnitude.

2 The L3 Detector

The L3 detector [10] consists of a central tracking chamber (TEC), a forward-backward tracking chamber (FTC), a high resolution electromagnetic calorimeter composed of bismuth germanium oxide (BGO) crystals with a barrel region and endcaps to cover the forward-backward solid angle down to 10°, a ring of scintillation counters, a uranium and brass hadron calorimeter with proportional wire chamber readout (which also comprises a barrel and forward-backward endcaps) and a high precision muon spectrometer. These detectors are located in a 12m diameter magnet which provides a uniform field of 0.5 T along the beam direction. Forward BGO arrays, on either side of the detector, measure the luminosity by detecting small angle Bhabha events.

The forward-backward tracking chamber and the BGO endcaps were not installed until 1991 and as a consequence 1990 data are limited to the barrel region $44^\circ < \theta < 136^\circ$. With the BGO endcaps and the FTC, we use data collected in the angular range $14^\circ < \theta < 166^\circ$ covering 97% of the full solid angle.

3 Event Selection

To select a $\gamma\gamma(\gamma)$ event we required:

(1) At least 70% of the center-of-mass energy to be in the BGO.

(2) The number of clusters in the BGO to be less than 9.

(3) The acollinearity angle between the two most energetic clusters to be less than 25°.

(4) No tracks detected inside TEC and FTC.

Cuts 1 and 2 eliminate all hadronic events and leave 1.2% $\tau^+\tau^-$ background, which is removed by cut 4. Cut 3 eliminates mainly cosmic ray background and low multiplicity noise events. Bhabha events, $e^+e^- \to e^+e^-(\gamma)$, constitute the main background which contaminates our data sample when both tracks remain undetected in the TEC and FTC. The probability to detect at least one of the two tracks, the veto efficiency, is measured for both the TEC and the FTC using Bhabha events with either one or two detected tracks. We used our hadronic sample to monitor the TEC performance and to exclude periods with low efficiency. Consequently the luminosity had to be corrected according to the number of hadronic events remaining in the data. Combining tracking information from the TEC ($|\cos(\theta)| < 0.883$) and the FTC ($0.883 < |\cos(\theta)| < 0.97$), we reach a veto efficiency of $99.98\% \pm 0.02\%$. With the above cuts we selected 426 candidates for an $e^+e^- \to \gamma\gamma(\gamma)$ reaction. The contamination from Bhabha background is estimated to be less than 3 events.

A special selection was performed for the three photon final state events. Keeping the previous cuts 1,2 and 4, we added the following ones:

(1) There must be at least 3 clusters in the BGO.

(2) The energy of the least energetic cluster must exceed 3 GeV.

(3) The angle in space between any two clusters must be larger than 25°.

(4) The sum of the angles in space between clusters must be more than 350°, thus ensuring that the event is highly coplanar.

With the above cuts we selected 10 $e^+e^- \to \gamma\gamma\gamma$ candidates.

4 Analysis

To take into account radiative corrections we used the Berends and Kleiss QED Monte Carlo [11] which includes virtual photon corrections, soft and hard bremsstrahlung to $O(\alpha^3)$. Figure 1(a) shows a comparison, between data and Monte Carlo, of the sum of energies of the two most energetic clusters normalized to the beam energy. Figure 1(b) shows a similar comparison for the acollinearity angle ζ, between the two most energetic clusters. The efficiency for selecting events with photons in the final state distributed according to the QED prediction was found to be $64\% \pm 3\%$ in the angular range $14^\circ < \theta < 166^\circ$ and $90\% \pm 1\%$ for $44^\circ < \theta < 136^\circ$. Losses from photon conversions, most significant in the forward-backward region, and from gaps in the detector are included. The trigger efficiency is more than 99.9%. The integrated luminosity for the different center-of-mass energies is given in Table 1. This table also shows the number of events for the 1990 and 1991 data runs and the total measured cross sections. The 1991 cross sections are also shown in Figure 2 as a function of the center-of-mass energy.

$\sqrt{s}$ (GeV)	$\mathcal{L}_{int}$ 1991 (pb^{-1})	$N_{\gamma\gamma(\gamma)}$ (1991)	σ_{meas} (pb) (1991)
88.5	0.20	2	-
89.4	0.59	15	40.2 ± 10.4
90.3	0.47	24	80.4 ± 16.4
91.2	7.52	278	58.0 ± 3.5
92.0	0.38	11	45.1 ± 13.5
93.0	0.72	25	54.5 ± 10.9
93.7	0.53	14	41.8 ± 11.2

$\sqrt{s}$ (GeV)	$\mathcal{L}_{int}$ 1990 (pb^{-1})	$N_{\gamma\gamma(\gamma)}$ (1990)	σ_{meas} (pb) (1990)
89.8	0.53	5	10.5 ± 4.7
91.2	2.59	43	18.4 ± 2.8
92.6	0.65	9	15.4 ± 5.1

Table 1: a) The integrated luminosities as a function of the center-of-mass energies for the 1991 data ($14^\circ < \theta < 166^\circ$). Also given are the number of events observed and the total measured cross sections.
b) The same table for the 1990 data ($44^\circ < \theta < 136^\circ$). The first and last three energy bins have been combined.

In Table 2 we give the measured differential cross sections for $e^+e^- \rightarrow \gamma\gamma(\gamma)$. Figure 3(a) shows the data points compared to the Born level and to the radiatively corrected QED cross section. We note that radiative corrections decrease the Born QED cross section in the barrel region while increasing it in the forward-backward region. The χ^2 of the data points compared to the QED expectation is 12.3 for 9 degrees of freedom, indicating that the measured differential cross section is in agreement with the QED prediction.

A possible QED breakdown has been parametrized in the differential cross section at Born level. As mentioned in the introduction the Lagrangian describing the coupling of an excited electron to a photon and an electron is gauge invariant but not renormalizable. As a consequence radiative corrections for the diagram involving the excited electron have not yet been calculated. Combining the QED contribution with corrections up to $O(\alpha^3)$ with the zeroth-order contribution of the excited electron leads to a differential cross section that is infrared divergent. The measured cross section compared to the theoretical one

$\lvert\cos\theta\rvert$	$N_{\gamma\gamma(\gamma)}$ (1990+1991)	$\left(\frac{d\sigma_{meas}}{d\Omega_{\gamma\gamma(\gamma)}}\right)$ (pb/sr) (1990+1991)
0.077	13	1.8 ± 0.5
0.177	23	3.3 ± 0.7
0.299	25	3.5 ± 0.7
0.435	18	2.6 ± 0.6
0.550	29	4.1 ± 0.8
0.658	52	8.2 ± 1.1
0.852	48	23.0 ± 3.3
0.906	38	28.2 ± 4.6
0.954	75	56.3 ± 6.5

Table 2: Differential cross sections as a function of $\lvert\cos\theta\rvert$ at $\sqrt{s} = 91.2$ GeV. The $\lvert\cos\theta\rvert$ values given in the first column are event-weighted averages; the second column gives the number of events. Data from 1990 ($44^\circ < \theta < 136^\circ$) and 1991 ($14^\circ < \theta < 166^\circ$) have been combined.

calculated to $O(\alpha^3)$ is:

$$\sigma(\theta)_{Measured} \;=\; \sigma(\theta)^{O(\alpha^3)}_{QED}\ (1\ +\ \rho)$$

where ρ is a measure of a possible QED breakdown. We approximated the infrared divergent differential cross section by a finite measurable one, replacing ρ by its Born level expression:

$$\rho \approx \left(\sigma(\theta)^0_T\ -\ \sigma(\theta)^0_{QED}\right)\ /\ \sigma(\theta)^0_{QED}\ =\ \delta_{new}$$

with δ_{new} as defined in the introduction. In this approach the data are directly compared to the theory.

We used the unbinned maximum likelihood method to set lower limits on the breakdown parameters and on the mass of an excited electron. The probability function was constructed by normalizing the differential cross section given above to the total cross section in our acceptance. The likelihood function is:

$$\mathcal{L} \;=\; \frac{1}{\sqrt{2\pi\sigma^2}}\ \exp\left(\frac{-(N_{obs} - N(\Lambda))^2}{2\sigma^2}\right)\ \prod_{i=1}^{N_{obs}} P(\theta_i, \Lambda)$$

where Λ is the parameter under consideration, N_{obs} the observed number of events, $N(\Lambda)$ the expected number of events, and $P(\theta_i, \Lambda)$ the event probability density depending on the parameter Λ and the polar event angle θ_i. The first term corresponds to the overall normalization constraint. The error σ on the number of expected events includes in quadrature the statistical error and a systematic error of 3%. At 95% confidence level we found $\Lambda_+ > 139$ GeV, $\Lambda_- > 108$ GeV. To fit the mass of the excited electron we used the full expression for the differential cross section given in reference 2, assuming the coupling constant $\lambda = 1$. The same likelihood function was used as for Λ_+ and Λ_-. At 95% confidence level we found $m_{e^*} > 127$ GeV. Figure 3(b) shows the ratio of measured to QED differential cross section. The solid curves illustrate the effect of Λ_+ and Λ_- on the QED prediction.

We searched for decays of $Z^0 \to \pi^0\gamma$, $Z^0 \to \eta\gamma$, $Z^0 \to \gamma\gamma$. To calculate the selection efficiency for these channels we used a $\pi^0\gamma$, $\eta\gamma$ Monte Carlo event simulation with particle angular distribution $(1+\cos^2\theta)$. The $\pi^0\gamma$, $\gamma\gamma$ decay modes leave the same photonic signature in the detector and the total acceptance for both was found to be 73%. The case of $Z^0 \to \eta\gamma$ is different because we only considered the decays of η into either $3\pi^0$ or 2γ which accounts for 71% of its decay products. The total acceptance for $Z^0 \to \eta\gamma$ was therefore found to be 52%. Table 3 lists the various processes and the total acceptances for the 1990 and 1991 data. In general the Born cross section at the Z^0 peak for the

Process	Acceptance×Efficiency	
	$44^\circ < \theta < 136^\circ$	$14^\circ < \theta < 166^\circ$
$Z^0 \to \pi^0\gamma,\ \gamma\gamma$	0.57	0.73
$Z^0 \to \eta\gamma$	0.40	0.52
$Z^0 \to \gamma\gamma\gamma$	0.30	0.49

Table 3: The acceptance×efficiency for the various processes in the two angular regions considered; the systematic error is 3%.

reaction $Z^0 \to X$ is given by:

$$\sigma_{peak} = \frac{12\pi}{m_Z^2}\,\frac{\Gamma_{ee}\,\Gamma_X}{\Gamma_Z^2}$$

where Γ_{ee} is the electronic width of the Z^0, Γ_Z the total Z^0 width and Γ_X the width of the rare decay mode under consideration. For the variation of the cross section with the center-of-mass energy we used a Breit Wigner formula with energy dependent width:

$$\sigma_s = \sigma_{peak}\,\frac{s\Gamma_Z^2}{(s-m_Z^2)^2 + \left(\frac{s\Gamma_Z}{m_Z}\right)^2}$$

For Γ_{ee}, Γ_Z and m_Z we used our measured values of reference 13. The likelihood constructed uses Poisson statistics to compare for every center-of-mass energy bin the observed and the expected number of events (contributions from QED to $O(\alpha^3)$ and from the Z^0 rare decays):

$$\mathcal{L} = \prod_{i=1}^{6} P(N_i, N_{exp}(\Gamma_X))$$

where N_i is the observed number of events for energy bin 'i' and N_{exp} is the expected number for that energy bin. A systematic error of 3% was taken into account. With this likelihood function we obtain at 95% confidence level the following upper limits:

$$\Gamma(Z^0 \to \eta\gamma) < 0.44 \text{ MeV or } \mathrm{BR}(Z^0 \to \eta\gamma) < 1.8 \times 10^{-4}$$

$$\Gamma(Z^0 \to \pi^0\gamma/\gamma\gamma) < 0.31 \text{ MeV or } \mathrm{BR}(Z^0 \to \pi^0\gamma) < 1.2 \times 10^{-4}$$

In composite models the Z^0 may couple to photons through its charged constituents [8]. The three photons in the final state coming from a Z^0 decay may be separated from the QED process $e^+e^- \to \gamma\gamma\gamma$ through their distinct topology. For example the energy of the least energetic photon for a QED event is preferentially low and it is emitted in the forward-backward direction. The cuts for three photon selection have been given above.

We found 10 events at all center-of-mass energies and from QED we expect 12 $e^+e^- \to \gamma\gamma\gamma$ events. Figure 4 shows the energy of the least energetic photon versus its angle with respect to the beam axis. We note here that the anomalous term which couples Z^0 to photons has negligible effect away from the Z^0 pole [8] and we therefore only considered events on the Z^0. The efficiency was calculated using an analytical calculation [8] which provides the $Z^0 \to \gamma\gamma\gamma$ cross section. The total acceptance was found to be 49%. We found 5 events on the Z^0 peak whereas from QED we expect 8.6. Using Poisson statistics and allowing for background, we set an upper limit on the branching ratio for the reaction $Z^0 \to \gamma\gamma\gamma$ of: $BR(Z^0 \to \gamma\gamma\gamma) < 3.3 \times 10^{-5}$.

5 Acknowledgements

We wish to express our gratitude to the CERN accelerator divisions for the excellent performance of the LEP machine. We acknowledge the effort of all engineers and technicians who have participated in the construction and maintenance of this experiment.

The L3 Collaboration:

O.Adriani,[14] M.Aguilar-Benitez,[23] S.Ahlen,[9] H.Akbari,[5] J.Alcaraz,[15] A.Aloisio,[25] G.Alverson,[10] M.G.Alviggi,[25] G.Ambrosi,[30] Q.An,[16] H.Anderhub,[42] A.L.Anderson,[13] V.P.Andreev,[34] T.Angelov,[13] L.Antonov,[37] D.Antreasyan,[7] P.Arce,[23] A.Arefiev,[24] A.Atamanchuk,[34] T.Azemoon,[3] T.Aziz,[8,1] P.V.K.S.Baba,[16] P.Bagnaia,[33] J.A.Bakken,[32] L.Baksay,[38] R.C.Ball,[3] S.Banerjee,[8] J.Bao,[5] R.Barillère,[15] L.Barone,[33] R.Battiston,[30] A.Bay,[17] F.Becattini,[14] U.Becker,[13,42] F.Behner,[42] J.Behrens,[42] S.Beingessner,[4] Gy.L.Bencze,[11] J.Berdugo,[23] P.Berges,[13] B.Bertucci,[30] B.L.Betev,[37,42] M.Biasini,[30] A.Biland,[42] G.M.Bilei,[30] R.Bizzarri,[33] J.J.Blaising,[4] B.Blumenfeld,[5] G.J.Bobbink,[15,2] M.Bocciolini,[14] R.Bock,[1] A.Böhm,[1] B.Borgia,[33] D.Bourilkov,[27] M.Bourquin,[17] D.Boutigny,[4] B.Bouwens,[2] E.Brambilla,[25] J.G.Branson,[35] I.C.Brock,[31] M.Brooks,[21] C.Buisson,[22] A.Bujak,[39] J.D.Burger,[13] W.J.Burger,[17] J.P.Burq,[22] J.Busenitz,[38] X.D.Cai,[16] M.Capell,[20] M.Caria,[30] G.Carlino,[25] F.Carminati,[14] A.M.Cartacci,[14] M.Cerrada,[23] F.Cesaroni,[33] Y.H.Chang,[13] U.K.Chaturvedi,[16] M.Chemarin,[22] A.Chen,[44] C.Chen,[6] G.M.Chen,[6] H.F.Chen,[18] H.S.Chen,[6] J.Chen,[13] M.Chen,[13] M.L.Chen,[3] W.Y.Chen,[16] G.Chiefari,[25] C.Y.Chien,[5] M.Chmeissani,[3] S.Chung,[13] C.Civinini,[14] I.Clare,[13] R.Clare,[13] T.E.Coan,[21] H.O.Cohn,[28] G.Coignet,[4] N.Colino,[15] A.Contin,[7] F.Crijns,[27] X.T.Cui,[16] X.Y.Cui,[16] T.S.Dai,[13] R.D'Alessandro,[14] R.de Asmundis,[25] A.Degré,[4] K.Deiters,[13] E.Dénes,[11] P.Denes,[32] F.DeNotaristefani,[33] M.Dhina,[42] D.DiBitonto,[38] M.Diemoz,[33] H.R.Dimitrov,[37] C.Dionisi,[33,15] M.T.Dova,[16] E.Drago,[25] T.Driever,[27] D.Duchesneau,[17] P.Duinker,[2] H.El Mamouni,[22] A.Engler,[31] F.J.Eppling,[13] F.C.Erné,[2] P.Extermann,[17] R.Fabbretti,[40] M.Fabre,[40] S.Falciano,[33] S.J.Fan,[36] O.Fackler,[20] J.Fay,[22] M.Felcini,[15] T.Ferguson,[31] D.Fernandez,[23] G.Fernandez,[23] F.Ferroni,[33] H.Fesefeldt,[1] E.Fiandrini,[30] J.Field,[17] F.Filthaut,[27] G.Finocchiaro,[33] P.H.Fisher,[5] G.Forconi,[17] T.Foreman,[2] K.Freudenreich,[42] W.Friebel,[41] M.Fukushima,[13] M.Gailloud,[19] Yu.Galaktionov,[24,13] E.Gallo,[14] S.N.Ganguli,[8] P.Garcia-Abia,[23] S.S.Gau,[44] D.Gele,[22] S.Gentile,[33,15] S.Goldfarb,[3] Z.F.Gong,[18] E.Gonzalez,[23] P.Göttlicher,[1] A.Gougas,[5] D.Goujon,[17] G.Gratta,[29] C.Grinnell,[13] M.Gruenewald,[29] C.Gu,[16] M.Guanziroli,[16] J.K.Guo,[36] V.K.Gupta,[32] A.Gurtu,[15,8] H.R.Gustafson,[3] L.J.Gutay,[39] K.Hangarter,[1] A.Hasan,[16] D.Hauschildt,[2] C.F.He,[36] T.Hebbeker,[1] M.Hebert,[35] G.Herten,[13] U.Herten,[1] A.Hervé,[15] K.Hilgers,[1] H.Hofer,[42] H.Hoorani,[17] G.Hu,[16] G.Q.Hu,[36] B.Ille,[22] M.M.Ilyas,[16] V.Innocente,[15,25] H.Janssen,[15] S. Jezequel,[4] B.N.Jin,[6] L.W.Jones,[3] A.Kasser,[19] R.A.Khan,[16] Yu.Kamyshkov,[28] P.Kapinos,[34,41] J.S.Kapustinsky,[21] Y.Karyotakis,[15,4] M.Kaur,[16] S.Khokhar,[16] M.N.Kienzle-Focacci,[17] W.W.Kinnison,[21] D.Kirkby,[29] S.Kirsch,[41] W.Kittel,[27] A.Klimentov,[13,24] A.C.König,[27] E.Koffeman,[2] O.Kornadt,[1] V.Koutsenko,[13,24] A.Koulbardis,[34] R.W.Kraemer,[31] T.Kramer,[13] V.R.Krastev,[37,30] W.Krenz,[1] A.Krivshich,[34] H.Kuitjen,[27] K.S.Kumar,[12] A.Kunin,[12,24] G.Landi,[14] D.Lanske,[1] S.Lanzano,[25] P.Lebrun,[22] P.Lecomte,[42] P.Lecoq,[15] P.Le Coultre,[42] D.M.Lee,[21] I.Leedom,[10] J.M.Le Goff,[15] R.Leiste,[41] M.Lenti,[14] E.Leonardi,[33] J.Lettry,[42] X.Leytens,[2] C.Li,[18,16] H.T.Li,[6] P.J.Li,[36] X.G.Li,[6] J.Y.Liao,[36] W.T.Lin,[44] Z.Y.Lin,[18] F.L.Linde,[15,2] B.Lindemann,[1] D.Linnhofer,[42] L.Lista,[25] Y.Liu,[16] W.Lohmann,[41,15] E.Longo,[33] Y.S.Lu,[6] J.M.Lubbers,[15] K.Lübelsmeyer,[1] C.Luci,[33] D.Luckey,[7,13] L.Ludovici,[33] L.Luminari,[33] W.G.Ma,[18] M.MacDermott,[42] P.K.Malhotra,[8,†] R.Malik,[16] A.Malinin,[4,24] C.Maña,[23] D.N.Mao,[3] Y.F.Mao,[6] M.Maolinbay,[42] P.Marchesini,[42] F.Marion,[4] A.Marin,[9] J.P.Martin,[22] L.Martinez-Laso,[23] F.Marzano,[33] G.G.G.Massaro,[2] T.Matsuda,[13] K.Mazumdar,[8] P.McBride,[12] T.McMahon,[39] D.McNally,[42] Th.Meinholz,[1] M.Merk,[27] L.Merola,[25] M.Meschini,[14] W.J.Metzger,[27] Y.Mi,[16] G.B.Mills,[21] Y.Mir,[16] G.Mirabelli,[33] J.Mnich,[1] M.Möller,[1] B.Monteleoni,[14] R.Morand,[4] S.Morganti,[33] N.E.Moulai,[16] R.Mount,[29] S.Müller,[1] A.Nadtochy,[34] E.Nagy,[11] M.Napolitano,[25] H.Newman,[29] C.Neyer,[42] M.A.Niaz,[16] A.Nippe,[1] H.Nowak,[41] G.Organtini,[33] D.Pandoulas,[1] S.Paoletti,[14] P.Paolucci,[25] G.Passaleva,[14,30] S.Patricelli,[25] T.Paul,[5] M.Pauluzzi,[30] F.Pauss,[42] Y.J.Pei,[1] D.Perret-Gallix,[4] J.Perrier,[17] A.Pevsner,[5] D.Piccolo,[25] M.Pieri,[15,14] P.A.Piroué,[32] F.Plasil,[28] V.Plyaskin,[24] M.Pohl,[42] V.Pojidaev,[24,14] N.Produit,[17] J.M.Qian,[3] K.N.Qureshi,[16] R.Raghavan,[8] G.Rahal-Callot,[42] G.Raven,[2] P.Razis,[26] K.Read,[28] D.Ren,[42] Z.Ren,[16] M.Rescigno,[33] S.Reucroft,[10] A.Ricker,[1] S.Riemann,[41] O.Rind,[3] H.A.Rizvi,[16] F.J.Rodriguez,[23] B.P.Roe,[3] M.Röhner,[1] S.Röhner,[1] L.Romero,[23] J.Rose,[1] S.Rosier-Lees,[4] R.Rosmalen,[27] Ph.Rosselet,[19] A.Rubbia,[13] J.A.Rubio,[15] H.Rykaczewski,[42] M.Sachwitz,[41] E.Sajan,[30] J.Salicio,[15] J.M.Salicio,[23] G.S.Sanders,[21] A.Santocchia,[30] M.S.Sarakinos,[13] G.Sartorelli,[7,16] M.Sassowsky,[1] G.Sauvage,[4] V.Schegelsky,[34] K.Schmiemann,[1] D.Schmitz,[1] P.Schmitz,[1] M.Schneegans,[4] H.Schopper,[43] D.J.Schotanus,[27] S.Shotkin,[13] H.J.Schreiber,[41] J.Shukla,[31] R.Schulte,[1] S.Schulte,[1] K.Schultze,[1] J.Schütte,[12] J.Schwenke,[1] G.Schwering,[1] C.Sciacca,[25] I.Scott,[12] R.Sehgal,[16] P.G.Seiler,[40] J.C.Sens,[15,2] L.Servoli,[30] I.Sheer,[35] D.Z.Shen,[36] S.Shevchenko,[29] X.R.Shi,[29] E.Shumilov,[24] V.Shoutko,[24] E.Soderstrom,[32] A.Sopczak,[35] C.Spartiotis,[5] T.Spickermann,[1] P.Spillantini,[14] R.Starosta,[1] M.Steuer,[7,13] D.P.Stickland,[32] F.Sticozzi,[13] H.Stone,[17] K.Strauch,[12] B.C.Stringfellow,[39] K.Sudhakar,[8,1] G.Sultanov,[16] R.L.Sumner,[32] L.Z.Sun,[18,16] H.Suter,[42] R.B.Sutton,[31] J.D.Swain,[16] A.A.Syed,[16] X.W.Tang,[6] L.Taylor,[10] C.Timmermans,[27] Samuel C.C.Ting,[13] S.M.Ting,[13] M.Tonutti,[1] S.C.Tonwar,[8] J.Tóth,[11] A.Tsaregorodtsev,[34] G.Tsipolitis,[31] C.Tully,[29] K.L.Tung,[6] J.Ulbricht,[42] L.Urbán,[11] U.Uwer,[1] E.Valente,[33] R.T.Van de Walle,[27] I.Vetlitsky,[24] G.Viertel,[42] P.Vikas,[16] U.Vikas,[16] M.Vivargent,[4] H.Vogel,[31] H.Vogt,[41] I.Vorobiev,[24] A.A.Vorobyov,[34] L.Vuilleumier,[19] M.Wadhwa,[16] W.Wallraff,[1] C.R.Wang,[18] G.H.Wang,[31] J.H.Wang,[6] Q.F.Wang,[12] X.L.Wang,[18] Y.F.Wang,[14] Z.M.Wang,[16,18] A.Weber,[1] J.Weber,[42] R.Weill,[19] T.J.Wenaus,[20] J.Wenninger,[17] M.White,[13] C.Willmott,[23] F.Wittgenstein,[15] D.Wright,[32] R.J.Wu,[6] S.X.Wu,[16] Y.G.Wu,[6] B.Wysłouch,[13] Y.Y.Xie,[36] Y.D.Xu,[6] Z.Z.Xu,[18] Z.L.Xue,[36] D.S.Yan,[36] X.J.Yan,[13] B.Z.Yang,[18] C.G.Yang,[6] G.Yang,[16] K.S.Yang,[6] Q.Y.Yang,[6] Z.Q.Yang,[36] C.H.Ye,[16] J.B.Ye,[18] Q.Ye,[16] S.C.Yeh,[44] Z.W.Yin,[36] J.M.You,[16] N.Yunus,[16] M.Yzerman,[2] C.Zaccardelli,[29] P.Zemp,[42] M.Zeng,[16] Y.Zeng,[1] D.H.Zhang,[2] Z.P.Zhang,[18,16] B.Zhou,[9] J.F.Zhou,[1] R.Y.Zhu,[29] H.L.Zhuang,[6] A.Zichichi,[7,15,16] B.C.C.van der Zwaan.[2]

1 I. Physikalisches Institut, RWTH, W-5100 Aachen, FRG§
III. Physikalisches Institut, RWTH, W-5100 Aachen, FRG§
2 National Institute for High Energy Physics, NIKHEF, NL-1009 DB Amsterdam, The Netherlands
3 University of Michigan, Ann Arbor, MI 48109, USA
4 Laboratoire de Physique des Particules, LAPP, F-74941 Annecy-le-Vieux, France
5 Johns Hopkins University, Baltimore, MD 21218, USA
6 Institute of High Energy Physics, IHEP, Beijing, P.R. China
7 INFN-Sezione di Bologna, I-40126 Bologna, Italy
8 Tata Institute of Fundamental Research, Bombay 400 005, India
9 Boston University, Boston, MA 02215, USA
10 Northeastern University, Boston, MA 02115, USA
11 Central Research Institute for Physics of the Hungarian Academy of Sciences, H-1525 Budapest 114, Hungary
12 Harvard University, Cambridge, MA 02139, USA
13 Massachusetts Institute of Technology, Cambridge, MA 02139, USA
14 INFN Sezione di Firenze and University of Florence, I-50125 Florence, Italy
15 European Laboratory for Particle Physics, CERN, CH-1211 Geneva 23, Switzerland
16 World Laboratory, FBLJA Project, CH-1211 Geneva 23, Switzerland
17 University of Geneva, CH-1211 Geneva 4, Switzerland
18 Chinese University of Science and Technology, USTC, Hefei, Anhui 230 029, P.R. China
19 University of Lausanne, CH-1015 Lausanne, Switzerland
20 Lawrence Livermore National Laboratory, Livermore, CA 94550, USA
21 Los Alamos National Laboratory, Los Alamos, NM 87544, USA
22 Institut de Physique Nucléaire de Lyon, IN2P3-CNRS/Université Claude Bernard, F-69622 Villeurbanne Cedex, France
23 Centro de Investigaciones Energeticas, Medioambientales y Tecnologicas, CIEMAT, E-28040 Madrid, Spain
24 Institute of Theoretical and Experimental Physics, ITEP, Moscow, Russia
25 INFN-Sezione di Napoli and University of Naples, I-80125 Naples, Italy
26 Department of Natural Sciences, University of Cyprus, Nicosia, Cyprus
27 University of Nymegen and NIKHEF, NL-6525 ED Nymegen, The Netherlands
28 Oak Ridge National Laboratory, Oak Ridge, TN 37831, USA
29 California Institute of Technology, Pasadena, CA 91125, USA
30 INFN-Sezione di Perugia and Universitá Degli Studi di Perugia, I-06100 Perugia, Italy
31 Carnegie Mellon University, Pittsburgh, PA 15213, USA
32 Princeton University, Princeton, NJ 08544, USA
33 INFN-Sezione di Roma and University of Rome, "La Sapienza", I-00185 Rome, Italy
34 Nuclear Physics Institute, St. Petersburg, Russia
35 University of California, San Diego, CA 92182, USA
36 Shanghai Institute of Ceramics, SIC, Shanghai, P.R. China
37 Bulgarian Academy of Sciences, Institute of Mechatronics, BU-1113 Sofia, Bulgaria
38 University of Alabama, Tuscaloosa, AL 35486, USA
39 Purdue University, West Lafayette, IN 47907, USA
40 Paul Scherrer Institut, PSI, CH-5232 Villigen, Switzerland
41 DESY-Institut für Hochenergiephysik, O-1615 Zeuthen, FRG
42 Eidgenössische Technische Hochschule, ETH Zürich, CH-8093 Zürich, Switzerland
43 University of Hamburg, W-2000 Hamburg, FRG
44 High Energy Physics Group, Taiwan, ROC
§ Supported by the German Bundesministerium für Forschung und Technologie
† Deceased.

References

[1] F.E. Low, Phys. Rev. Lett. **14** (1965) 238 ;
R. P. Feynman, Phys Rev. Lett. **74** (1948) 939 ;
F. M. Renard, Phys Lett. **116B** (1982) 264.

[2] A. Litke, Harvard Univ., Ph.D Thesis (1970) unpublished.

[3] S. Drell, Ann. Phys. (N.Y.) **4** (1958) 75.

[4] C. N. Yang, Phys. Rev. **77** (1950) 242.

[5] M. Jacob,T. T. Wu, Phys. Lett. **232B** (1989) 529 ;
G. B. West, Mod. Phys. Lett. **5A** No. 27 (1990) 2281 ;
S. Ghosh, D. Chatterjee, Mod. Phys. Lett. **5A** No. 19 (1990) 1493.

[6] See "Rare Decays", I.J. van der Bij and E.W.N. Glover (Conveners), in Z Physics at LEP 1, CERN Yellow Book, 1989, edt by Altarelli, R. Kleiss and C. Verzegnassi.

[7] F. M. Renard, Phys. Lett. **116B** (1982) 269 ;
M. Bardadin-Otwinowska, CERN-PPE/92-6 (1992).

[8] M. Baillargeon, F. Boudjema,"New Physics Through Final State Photons", to be published, CERN-Yellow-Book "Photon Radiation from Quarks"

[9] L3 Collab., B. Adeva et al., Phys. Lett. **250B** (1990) 199.

[10] L3 Collab., B. Adeva et al., Nucl. Instr. and Meth. **A289** (1990) 35.

[11] F.A. Berends and R. Kleiss, Nucl. Phys. **186B** (1981) 22.

[12] ALEPH Collab., D. Decamp et al., (1991) CERN-PPE/91-149 ;
DELPHI Collab., P.Abreu et al., Phys. Lett. **268B** (1991) 296 ;
OPAL Collab., M. Z. Akrawy et al., Phys. Lett. **257B** (1990) 531.

[13] L3 Collab., B. Adeva et al., Z. Phys. **51C** (1991) 179.

Figure Captions

Figure 1: a) The sum of energies of the first and second most energetic photons divided by the center-of-mass energy. b) The acolinearity angle ζ, between the two most energetic photons.

Figure 2: Total measured cross section as a function of the center-of-mass energy for the angular region $14^\circ < \theta < 166^\circ$. QED includes virtual and radiative corrections to $O(\alpha^3)$.

Figure 3: a) Measured differential cross section. The solid line gives the QED differential cross section to $O(\alpha^3)$; the dashed line the zero-order QED differential cross section. b) Ratio of measured to QED differential cross sections. We superimpose the same ratio with contributions from QED to $O(\alpha^3)$ and from Λ_+, Λ_- using the lower limits found.

Figure 4: The energy of the least energetic photon versus its angle with respect to the beam axis.

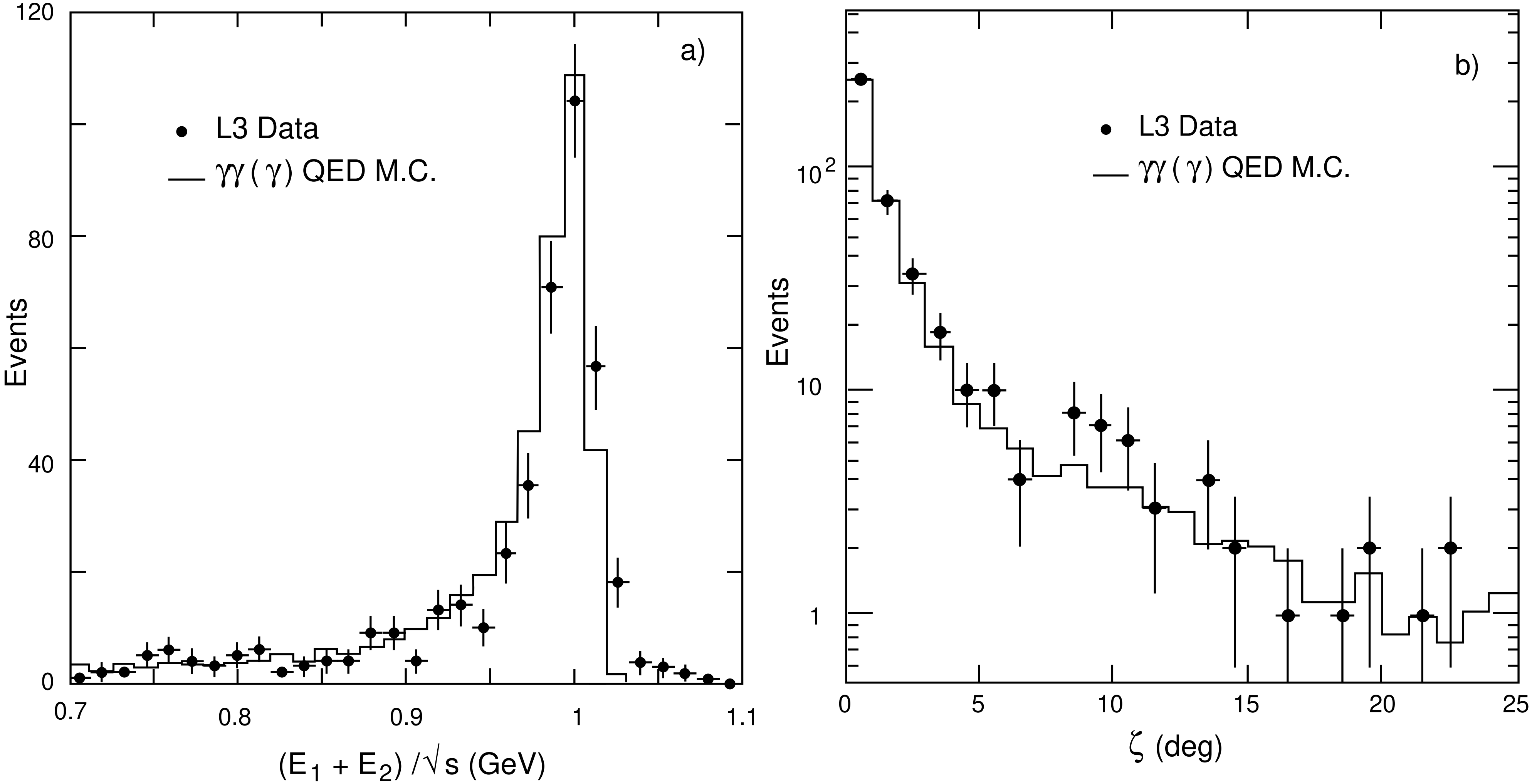

120
80
40
0
Events
a)
L3 Data
γγ(γ) QED M.C.
0.7
0.8
0.9
1
1.1
(E1 + E2) /√s (GeV)
b)
Events
10^2
10
1
0
5
10
15
20
25
ζ (deg)

Figure 1

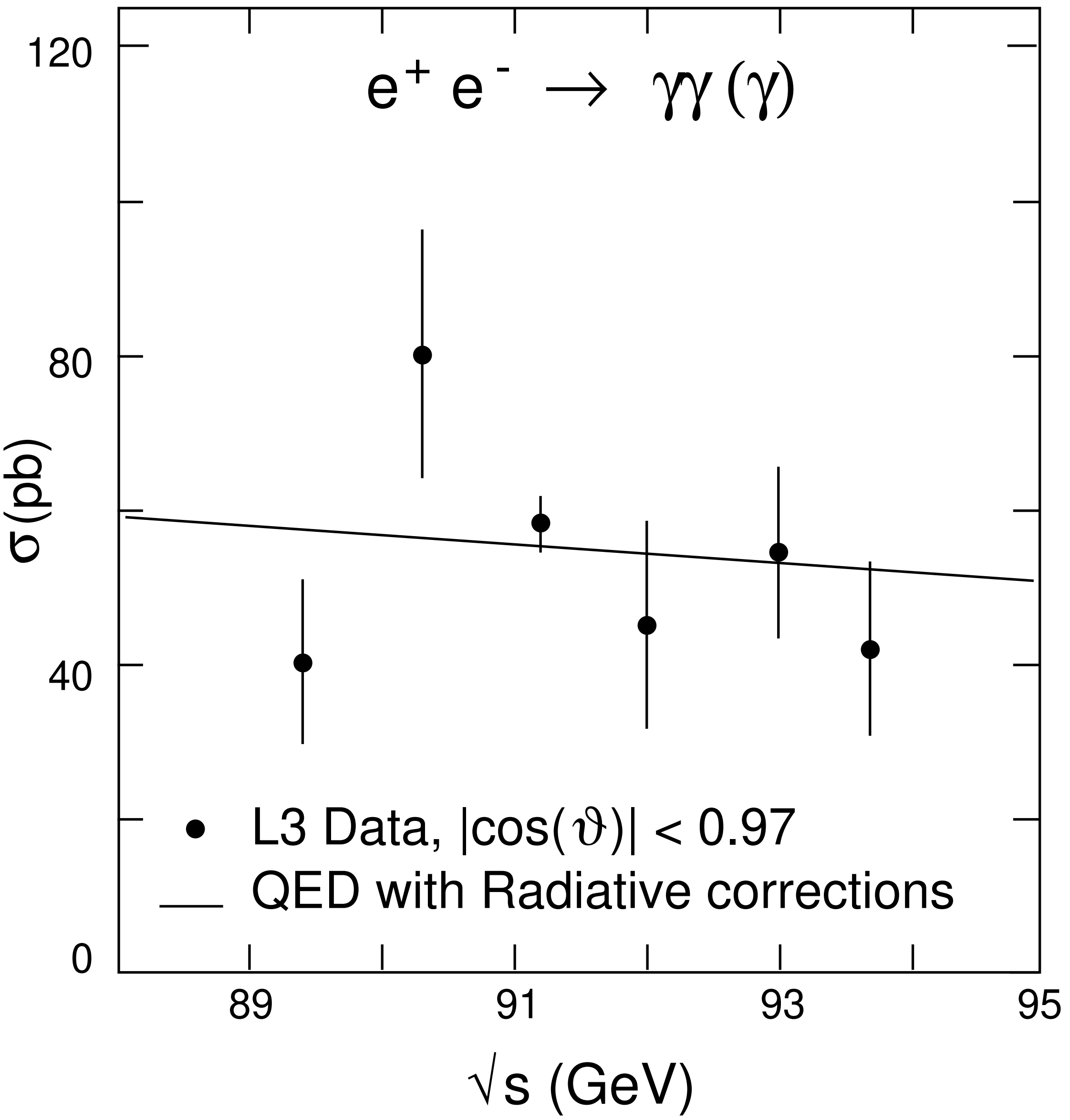
$e^+ e^- \to \gamma\gamma(\gamma)$
120
80
40
0
σ(pb)
89
91
93
95
√s (GeV)
L3 Data, $|\cos(\vartheta)| < 0.97$
QED with Radiative corrections

Figure 2

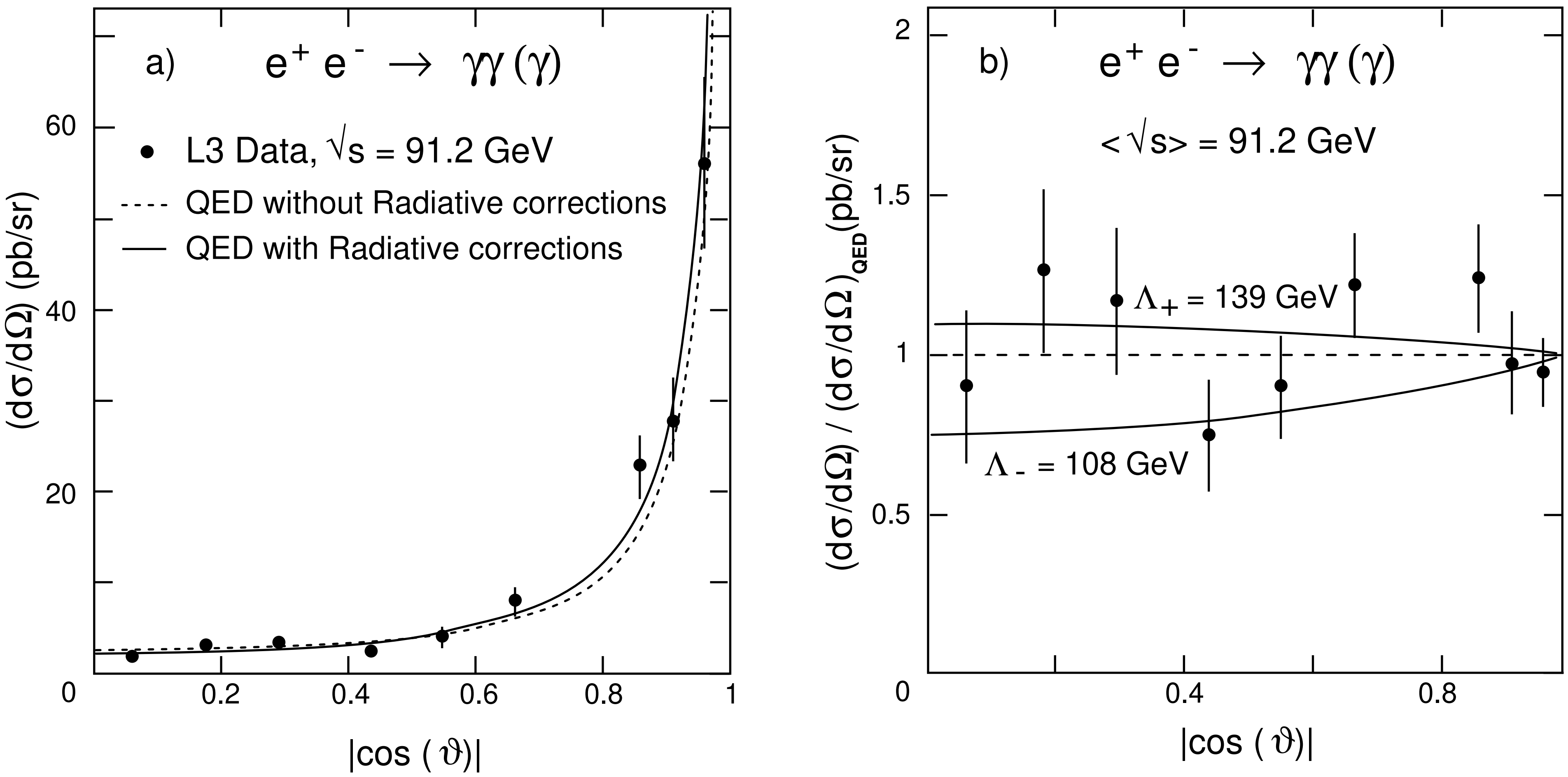

a)
$e^+ e^- \to \gamma\gamma(\gamma)$
L3 Data, $\sqrt{s}$ = 91.2 GeV
QED without Radiative corrections
QED with Radiative corrections
$(d\sigma/d\Omega)$ (pb/sr)
0
20
40
60
0.2
0.4
0.6
0.8
1
$|\cos(\vartheta)|$
b)
$e^+ e^- \to \gamma\gamma(\gamma)$
$<\sqrt{s}>$ = 91.2 GeV
Λ_+ = 139 GeV
Λ_- = 108 GeV
$(d\sigma/d\Omega)$ / $(d\sigma/d\Omega)_{QED}$(pb/sr)
0
0.5
1
1.5
2
0.4
0.8
$|\cos(\vartheta)|$

Figure 3

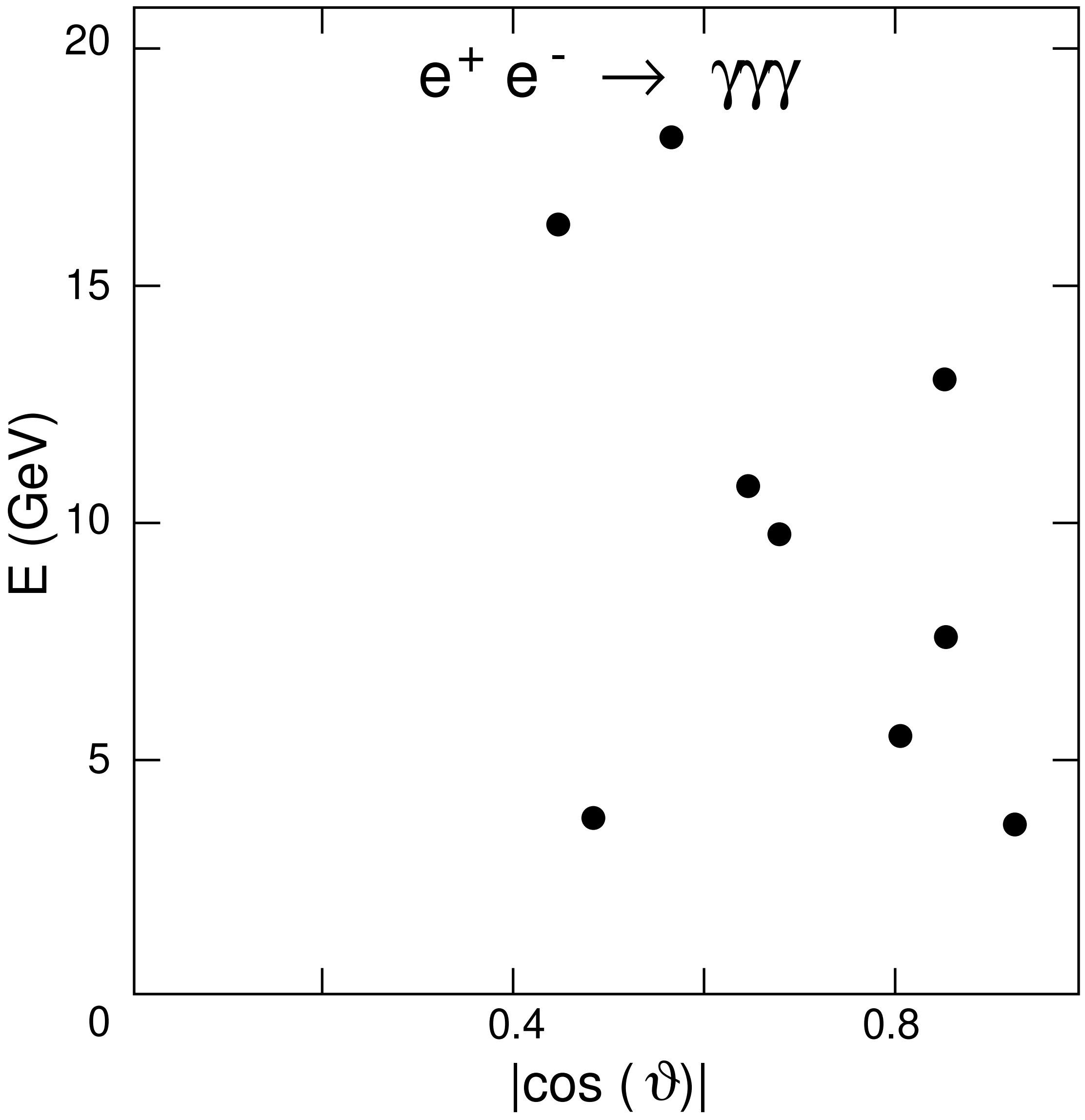

$e^+ e^- \rightarrow \gamma\gamma\gamma$
20
15
10
5
0
E (GeV)
0.4
0.8
|cos (ϑ)|

Figure 4